

RESEARCH ARTICLE

The Influence of External CFRP String Reinforcement on The Behavior of Flexural RC Elements

Junaedi Utomo^{1*}, Nauval Rabbani², Sri Tudjono³, Han Aylie³, Sukamta³

¹Department of Civil Engineering, Atma Jaya Yogyakarta University, Yogyakarta, Indonesia.

²Master Program in Civil Engineering, Diponegoro University, Semarang, Indonesia.

³Department of Civil Engineering, Diponegoro University, Semarang-Indonesia.

* Corresponding author : junaedi.utomo@ujay.ac.id
Tel.: +62811268405
Received: Oct 12, 2020; Accepted: Aug 16, 2021.
DOI: 10.25299/jgeet.2021.6.3.5685

Abstract

External reinforcement is an excellent method for improving the load carrying capacity and ductility behaviour of reinforced concrete members in flexure. Enhancement becomes a necessity when current standards mandate a higher performance compared to older codes. External reinforcement is an environmentally friendly and sustainable solution, since demolition and re-building could be postponed, and the building can be used while work is conducted on the members. Carbon Fiber Reinforced Polymers (CFRP), having a low weight-to-volume ratio and an excellent resistance to corrosion, can be used as external reinforcement to effectively increase the flexural and shear strength of a member. To evaluate the effectiveness of CFRP strings, two types of reinforced concrete T-beams were tested. The specimens consist of a strengthened member in both shear and flexure using CFRP wraps and CFRP strings, and a conventional reinforced concrete beam. The specimens were subjected to a one-point-loading system to simulate high shear stresses in combination with a maximum bending moment at mid-point. The installation of CFRP strings was conducted using the Near Surface Mounted (NSM) method, while the sheets were Externally Bonded Reinforcement (EBR). The strings and sheets were impregnated and pultruded on side. The test results showed that the strings and wraps substantially increased the ultimate load carrying capacity and ductility of the member. The ultimate load enhancement was found to be 32% from 117kN to 154kN, and the vertical deformation improved 25% from 16 mm to 20 mm. The failure mode was characterized by initial debonding of the strings in the interface between the strings and the epoxy, followed by string-rupture. The two strings ruptured concurrently, due to stress re-distribution within the member.

Keywords: External Strengthening, Carbon Fiber Reinforced Polymer (CFRP), Flexure, load-carrying capacity.

1. Introduction

The requirements for seismic design changes, as it is influenced by the shifting of earthquake zone mapping. Existing reinforced concrete flexural members therefore requires re-evaluation and, most probably, improvements in terms of their load-carrying capacity. To achieve this goal, an element might necessitate additional reinforcement or external strengthening. Among the methods of steel jacketing and section enlargement, external strengthening using Carbon Fiber Reinforced Polymer (CFRP) provides a simple and less invasive technique to enhance the load-carrying capacity of a member. Structural strengthening using CFRP as external reinforcement is proven to be effective for seismic rehabilitation of structures over the past decades (Mugahed Amran et al., 2018). Carbon fiber FRP is chosen for this experiment considering the advantages as compared to other fibers such as aramid and glass. These advantages are: very high strength, lightweight, corrosion resistance, and the ease in application. CFRP is widely used for strengthening of concrete structures (El Gamal et al., 2019).

In terms of CFRP application, two methods are available; the first being the Externally Bonded Reinforcement (EBR) and secondly, the Near Surface Mounted (NSM) method. The EBR method can be applied for shear and flexural strengthening, the types of CFRP that are commonly assessed are sheets and laminates. The characteristics of this method are that the CFRP is attached entirely to the outer concrete surface using an epoxy resin or bonding agent. The concrete surface usually requires

grinding prior to application of the CFRP. The compatibility between the concrete member and the CFRP is dependent on the performance of the interface between the epoxy and the concrete, and the epoxy and CFRP. The concrete, therefore, has to meet a minimum compressive strength to ensure that rupture in the concrete adjacent to the bond-area will not occur. Research has been conducted to investigate the flexural response of CFRP strengthened members based on the EBR method. It was found that the use of wrap-type CFRP increased the flexural capacity up to 45%, while debonding between the CFRP and epoxy resin was the failure mode (Tudjono et al., 2015). This mode of failure was reported by other researchers, concluding that especially for EBR, debonding becomes the most likely failure mode (Breña et al., 2003; Kotynia et al., 2008; Shin and Lee, 2003).

The NSM method, on the other hand, per definition provides a better bond performance since the CFRP is fully or partially embedded in the concrete near the surface of the member. The application of NSM requires the implantation of the CFRP within the concrete member; a groove needs to be constructed near the concrete surface, deep enough to house the CFRP member. From the point of view of application, rods, bars or plates could be used. The NSM method is mainly utilized for flexural strengthening. One of the major advantages of this system is that debonding can be prevented. Experiments on the NSM bond performance have previously been carried out to illustrate the capacity and failure behavior based on the direct pull-out and shear pull-out tests (Budipriyanto et al., 2018; Han

et al., 2018; Lee et al., 2013; Soliman et al., 2011). The results showed that the parameters affecting the bond behavior are: the concrete strength, groove depth, the type of epoxy material, the embedment length, and characteristics of the CFRP material. Additionally, experiments of beams under static loading (Bilotta et al., 2011; Dias et al., 2018; Tudjono et al., 2018) provided a picture of the failure behavior of NSM members. All results revealed that in general the NSM provides a better bond performance compared to the EBR.

In this study, CFRP carbon strings were utilized as flexural strengthening, based on the dry lay-up NSM system, in combination with shear strengthening using the sheets wet lay-up EBR method. The experiment focused on the effectiveness of the composite element in terms of load-carrying capacity enhancement and the failure behavior at ultimate. The specimens were T-sections in bending based on the experiments conducted by (Tudjono et al., 2015) and (Sapulete, 2018). The results were compared to an identical specimen having the same dimensions and material properties, without the CFRP external reinforcements.

Comparing the two systems, the significant disparity is in the fibers-resin interaction. For the wet lay-up EBR method, a layer of epoxy resin is attached to the concrete surface, and on top of this layer, the CFRP sheets are placed. An additional layer of the same resin is brushed into the sheets. The strings using the NSM method were based on the dry lay-up method; the strings were pre-impregnated (pre-preg) before placed into the concrete. A different type of epoxy resin is used for this purpose, and the main objective is to enhance the absorbance of resin into the fibers. Pre-preg is customarily performed at the manufacturing plant but could also be conducted on-site. The disadvantage of the latter is that the impregnation process is not as perfect as in the plant, and the geometry of cross-section will more likely be non-uniform.

2. Research Objective

The objective of this study is to analyze the effectiveness and influence of external reinforcement using a combination of shear and flexural CFRP reinforcement. The sheets are utilized as external shear reinforcement, and strings were used for improving the load carrying capacity and ductility of the member. The string will provide additional tensile force in the tensile area of the beam, and the sheets enhance the shear capacity while simultaneously producing a confined condition to the concrete in compression zone.

The behavior of the reinforced member is studied through the crack load and ultimate load levels, while the vertical deformation was measured at first concrete cracking and at ultimate. The comparison of these data to the control element without external reinforcement is used for analyzes. Further, the failure mode and crack propagation are visually observed to explain the data outcome and failure phenomenon. Further, the failure mode deviation to the reinforced concrete member without external reinforcement is studied, and the behavior of

strings are investigated to provide possible improvements both for the producer and the applicator at the field.

3. Specimen Specifications and External Strengthening

The experimental study included three T-beams sections with a length of 2500 mm. The specimens were simply supported with a clear span of 2300 mm. The elements were tested monotonically, with a one-point loading system applied at mid-span. An increment load of 20 kN/minute was applied on the member till failure (Fig. 1). One conventional reinforced beam was produced and numerated as BC. This element functioned as a controlling element and as a comparison instrument to the two CFRP reinforced members denoted as BS1 and BS2. The section dimensions and conventional steel reinforcements are shown in Fig. 2a. The concrete had a 28-day cylindrical compression strength (f'_c) of 38.4 MPa, and the 19 mm tensile steel reinforcement had a yield strength (f_y) of 433 MPa. The 16 mm compression reinforcement had a yield strength (f_y) of 416 MPa. Ø6 mild steel bars with a distance of 250 mm apart were used as stirrups. The elastic modulus of elasticity was 200 GPa.

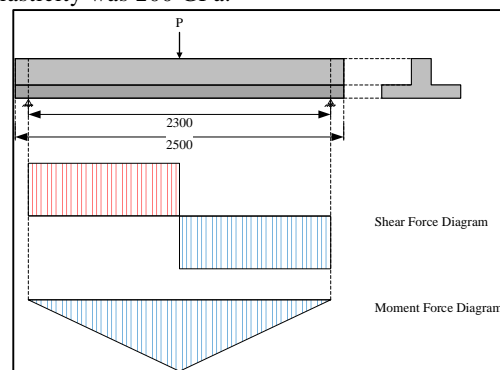


Fig 1. Specimen Specification and Loading System

The specimens BS were externally reinforced in shear and flexure. The shear reinforcement was applied on the web of the member using the so-called U configuration based on the EBR method. CFRP sheets with widths of 100 mm were placed with a distance of 30 mm (Fig. 2 and Fig. 3). The section as seen in Fig. 2a is the controlling element, designed based on the older codes, without external CFRP reinforcement while Fig. 2b is the cross section of the specimen with the two CFRP string reinforcements situated at the tensile area of the T-section.

The CFRP sheets were unidirectional woven carbon fiber fabrics with a thickness of 0.129 mm. The composite material had a tensile strength of 4.3 GPa and a tensile modulus elasticity of 225 GPa in combination with an ultimate 1.91% elongation. The sheet consists of one layer applied by the wet lay-up process. The epoxy resin functioning as bonding agent was thixotropic epoxy-based impregnating resin.

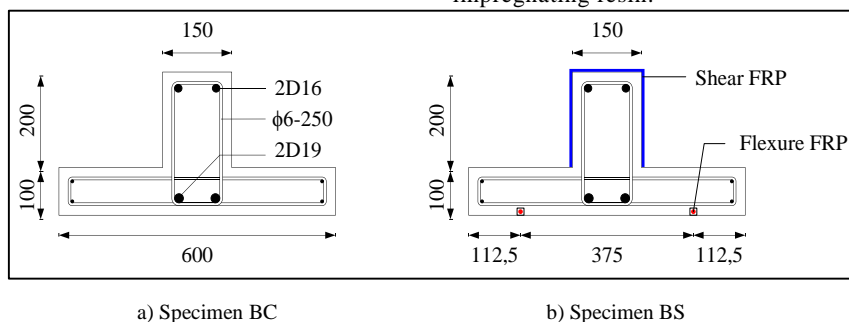


Fig 2. Cross-Section Details and Specifics

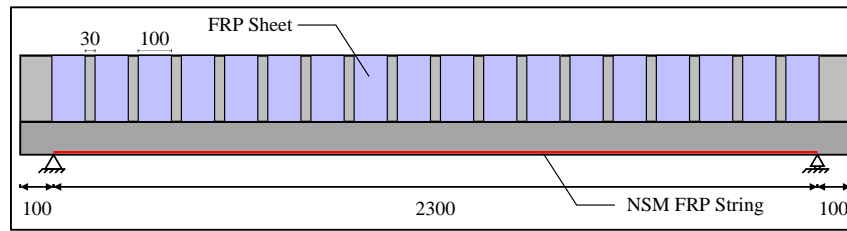


Fig 3. Details of External Shear CFRP Reinforcement

For the flexural reinforcements, CFRP strings were used (Fig. 4a). The strings were impregnated with an epoxy resin agent and pultruded (Fig. 4b). CFRP strings are unidirectional carbon fibers with a tensile strength of 4 GPa and a tension modulus of elasticity of 240 GPa in combination with an ultimate strain of 1.6%. The approximate diameter of pultruded strings was measured to be 10 mm with a tensile strength of 2 GPa and a tension modulus of elasticity of 230 GPa. The mechanical

properties of the sheets and string were similar except for the ultimate tensile strength. Contradictory to the shear reinforcements, the strings were attached to the extreme tensile concrete fibers using the NSM method. A different type of resin from the resin used for impregnation purposes was used to attach the strings into the groove. The strings were situated on the tensile part of the section, i.e. the flange. Two longitudinal strings with a distance of 375 mm were used (Fig. 2b).



Fig 4. CFRP String Details and Pultrusion

The sequence of the NSM strings was as follows: a groove with a width and depth of 1.5 times the string diameter was prepared; the groove was cleaned throughout by sandblasting and kept dry; the strings were impregnated and pultruded to straighten the individual fibers in the longitudinal direction; a layer of the bonding resin was placed in the groove, followed by the strings; the strings were pushed towards the bottom of the groove, and the gap was further filled with the bonding resin (Fig. 5); the surface was leveled and the resin was allowed to cure.

4. Experimental Research

The experimental setup is shown in Fig. 6. To induce a negative moment to simulate the position of the beam near the beam-column joint, the specimens were turned over with the flange on the bottom of the member. This has a practical reason since it is far simpler to induce a force downwards within the loading frame. This method has been used in previous research by (Sapulete, 2018; Tudjono et al., 2018, 2015). A load cell type CLC-500KNA with a capacity of 500 kN was used to record the monotonic load increment produced by the hydraulic jack with an increment rate of 20kN per minute. The increment was reduced to 10kN approaching the ultimate design load. Two displacement transducers with type CDP-100MT and a sensitivity of 100×10^{-6} strain/mm and maximum capacity of 100 mm were used to record the displacement during the loading sequences. The two transducers were situated on both sides of the web as can be seen in Fig. 7 and demonstrated in Fig. 6. All data were digitalized using a data logger. To monitor the horizontal movements of the specimens, a displacement transducer with type CDP-25M and a sensitivity of 500×10^{-6} strain/mm and maximum capacity of 100 mm was placed at mid-point, horizontally at the center of gravity of the section's member.



Fig 5. NSM String Placement

The concrete strength was obtained from six cylinders with a dimension of 100 by 200 mm that were prepared simultaneously during the production of the T-beam specimens. The cylinders were kept moist by submerging them, and then were dried. The T-beam specimens were cured by using a wet blanket during the 28-day period. Additional data such as temperature, humidity and the specimens' physical irregularities were recorded and used as secondary data when applicable.

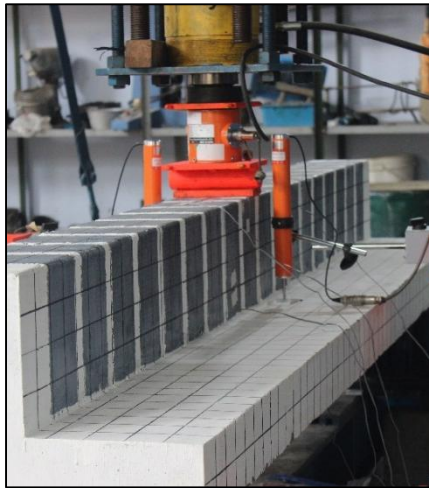


Fig 6. Loading Test

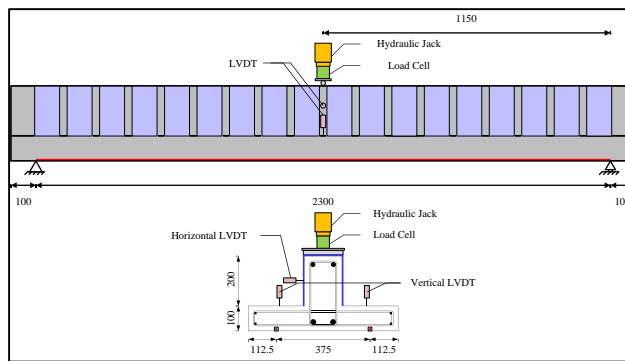


Fig 7. Experimental Setup

5. Results and Discussion

5.1. Load carrying capacity

Based on the experimental data, a summary of results is reported in Table 1. The data consist of the load magnitude when the first crack in the concrete in tension (P_{crack}) appeared and the ultimate load (P_{max}) and the corresponding vertical displacements (Δ_{crack} and Δ_{max}). Since the deviation of test results between BS21 and BS2 were small, the average values were presented. All data were recorded at mid-span area of the beam.

Table 1. Experiment Data

Code Name	P_{crack} (kN)	P_{max} (kN)	Δ_{crack} (mm)	Δ_{max} (mm)
BC	29.01	116.87	1.37	20
BS	36.02	154.36	1.87	16

In Fig. 8 the internal force equilibrium comparison is presented. The BC specimen's capacity is a contribution of the concrete and steel in compression and the steel in tension. The reinforced section has an additional force component that originated from the CFRP strings situated at the extreme tensile fibers. The amount of this external reinforcement should take into account the shifting of the neutral axis, so that the failure mode will remain as under-reinforced.

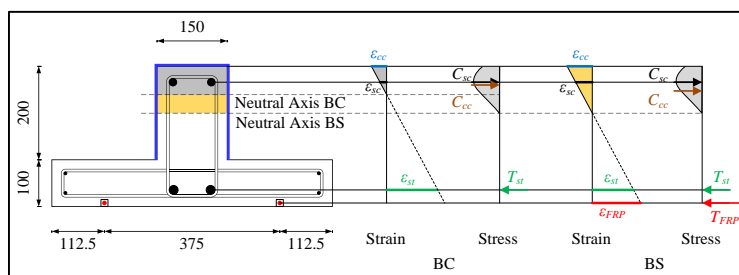


Fig 8. Internal Vector Component Comparison

5.2. Crack pattern and failure modes

The final crack pattern of BC and BS is shown in Fig. 9. Specimen BC unmistakably failed in flexure. Vertical cracks started at mid-span in the tension zone and propagated vertically towards the neutral axis of the section. This confirms

that the flexure stresses dominated the failure behavior in this region. Secondary vertical cracks appeared adjacent to this first crack, and as the first crack widened, the secondary cracks grew both in length and width towards the intersection between the web and the flange. From here on, these cracks started to

deviate from their vertical path, and diverge with an angle of approximately 45-degrees inwards, as can be seen clearly in Fig. 9a.

The specimens BS showed an initial flexure crack at mid-span; the secondary cracks were more evenly distributed as compared to BC (Fig. 9b). As was the case of BC, the cracks deviated into shear cracks, but contradictory to BC, these cracks started to diverge into shear cracks even in the flange area. When cracks became wider, the tensile steel yielded, resulting

in the crushing of concrete in the compression zone. The element lost its internal force equilibrium and the large strain disparities in the interface between the epoxy and concrete resulted in debonding at around the mid-point area. The vertical deformation of the member increased rapidly, since the remaining CFRP bond at the far end of the beams was the only internal force component counteracting the external load. Finally, the CFRP strings ruptured and the tests were terminated (Fig. 10).

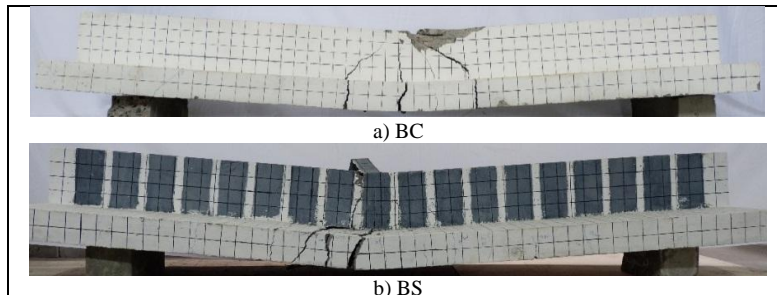


Fig 9. Crack Pattern at Failure

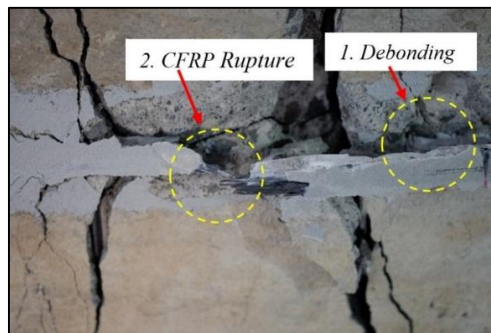


Fig 10. Failure Mode: (1) Epoxy Debonding and (2) CFRP Rupture

5.3. Analysis

The strengthened members have a substantially better performance in terms of load-carrying capacity. The members BS had a 33% capacity improvement when compared to the control element BC. The context of this increase originated from the additional tensile component provided by the CFRP strings and the enhancement in concrete compression strength due to the confinement endowed by the shear reinforcement. The increase in concrete compression strength due to shear reinforcement was studied by [Aylie et al., \(2015\)](#), [Huang et al., \(2018\)](#), and [Bouamra and Ait Tahar, \(2017\)](#). The combination of the additional tension component provided by the CFRP strings, and concrete confinement in the compression area, resulted in an increase in the internal moment, and thus an improvement in load-carrying capacity (Fig. 8).

As for the load level at which the first crack appeared, it can be seen that the cracking load for BS is 24% higher as compared to BC. The cracking moment depends on the tensile strains in the extreme concrete fibers, which in turn is a function of the beam's curvature. The curvature is influenced positively by the stiffness of the member. The stiffness of specimens BS was improved by the presence of the strings, which have a noticeably higher elastic modulus when compared to the concrete. The confined concrete in the compression zone also added to the stiffness of the section. After the concrete cracked, the bond between the strings and concrete remained intact and controlled the deformation of the member through the shear strength that prevented the propagation of cracks in the tension zone to a certain degree. A state of internal prestressing was induced in these extreme tension layers, explaining the lesser

vertical displacement at ultimate. The observation of the strings revealed that the bond at the far ends of the beams was maintained up till failure.

The crack pattern of BC is strongly influenced by the flexure mode. The first crack at mid-span is vertical and distinctively caused by high flexure stresses and strains. The secondary cracks, on the other hand, are initiated by flexure stresses in the extreme tensile fibers of the flange, but reaching the junction between the flange and the web, the section width becomes significantly smaller. This, in combination with a reduced bending moment that can be seen in Fig. 1, resulted in the domination of shear stresses and explains the circa 45-degree crack deviation. The collapse of the member is categorized as under-reinforced flexure.

The specimens BS failed due to a combination of flexure-shear stresses; this was concluded from the deviation in crack angle that occurred in the flanges. The secondary cracks were distributed more evenly, with a closer distance apart. The presence of the CFRP strings prevented the formation of large cracks, the yielding process of the conventional steel was prolonged and enabled the cracks to distribute more evenly. The combination of flexure-shear cracks in the flanges resulted due to the fact that only the web, and not the flange, was externally reinforced with the CFRP sheets. The bond within the CFRP string interface remained integral up till the crushing of the concrete in compression, and debonding started at the center part of the beam. The remaining bond at the far ends produced high stresses in the strings that finally ruptured.

6. Conclusion

The study looked into the behavior of externally reinforced flexural members using CFRP elements. The sheets were wet lay-up and were used as shear reinforcement based on the EBR method. The strings were dry lay-up and equipped as flexural reinforcement in the tensile area based on the NSM approach. The test results concluded that a combination of external shear and flexure reinforcement can significantly improve both the load-carrying capacity and the deformation behavior. The enhancement in flexural strength is mainly a contribution of the internal force equilibrium improvement that originated from the CFRP in the tension zone, and the increase in concrete compression strength is a result of confinement from the shear reinforcement. It is interesting to study to which degree the contribution of both these factors are, since the amalgamation of these two methods also shifted the failure mode from under-reinforced flexure to under-reinforced flexure-shear.

The two external reinforcements also influenced the member's stiffness positively. The vertical deformation of the member was reduced substantially, even under increasing load levels. The load levels at which the first crack occurs was controlled by the presence of the tensile CFRP reinforcement. The extended first cracking has an affirmative effect on conventional steel corrosion control. The test results suggested that the BS member could still be categorized as under-reinforced, but since the failure mode was a product of many additional factors, this cannot be seen as a general failure mode. The crack distribution was also more evenly distributed, with less crack-widths, which has a positive impact on controlling environmental influences such as humidity and possible chemical components to both concrete and conventional reinforcement.

In a nutshell, the proposed system is sufficient in rejuvenating an under-capacitated member with minimal effort. The system is best used for low-rise and medium-rise buildings.

Acknowledgment

The authors would like to acknowledge PT. SIKA Indonesia, the Structural and Material Laboratory of the Diponegoro University and the research cooperation between Nihon University in Japan, Atma Jaya University in Yogyakarta and Diponegoro University in Semarang.

References

Aylie, H., Antonius, Okiyarta, A.W., 2015. Experimental study of steel-fiber reinforced concrete beams with confinement. *Procedia Eng.* 125, 1030–1035. <https://doi.org/10.1016/j.proeng.2015.11.158>

Bilotta, A., Ceroni, F., Di Ludovico, M., Nigro, E., Pecce, M., Manfredi, G., 2011. Bond Efficiency of EBR and NSM FRP Systems for Strengthening Concrete Members. *J. Compos. Constr.* 15, 757–772. [https://doi.org/10.1061/\(asce\)cc.1943-5614.0000204](https://doi.org/10.1061/(asce)cc.1943-5614.0000204)

Bouamra, Y., Ait Tahar, K., 2017. Mechanical performance of a confined reinforced concrete beam. *Procedia Struct. Integr.* 5, 155–162. <https://doi.org/10.1016/j.prostr.2017.07.086>

Breña, S.F., Bramblett, R.M., Wood, S.L., Kreger, M.E., 2003. Increasing Flexural Capacity of Reinforced Concrete Beams Using Carbon Fiber-Reinforced Polymer Composites. *ACI Struct. J.* 100, 34–46.

Budipriyanto, A., Han, A.L., Hu, H.T., 2018. Bond-shear Behavior of FRP Rods as a Function of Attachment Configuration. *J. Adv. Civ. Environ. Eng.* 1, 9–17. <https://doi.org/10.30659/jacee.1.1.9-17>

Dias, S.J.E., Barros, J.A.O., Janwaen, W., 2018. Behavior of RC beams flexurally strengthened with NSM CFRP laminates. *Compos. Struct.* 201, 363–376. <https://doi.org/10.1016/j.compstruct.2018.05.126>

El Gamal, S.E., Al Nuaimi, A., Al-Saidy, A., Al-Shanfari, K., 2019. Flexural behavior of RC beams strengthened with CFRP sheets using different strengthening techniques. *J. Eng. Res.* 16, 35–43. <https://doi.org/10.24200/tjer.vol16iss1pp35-43>

Han, A., Gan, B.S., Budipriyanto, A., 2018. Shear-bond behavior of fiber reinforced polymer (FRP) rods and sheets, in: *MATEC Web of Conferences*. pp. 1–7. <https://doi.org/10.1051/mateconf/201819502001>

Huang, L., Zhang, C., Yan, L., Kasal, B., 2018. Flexural behavior of U-shape FRP profile-RC composite beams with inner GFRP tube confinement at concrete compression zone. *Compos. Struct.* 184, 674–687. <https://doi.org/10.1016/j.compstruct.2017.10.029>

Kotynia, R., Baky, H.A., Neale, K.W., Ebead, U.A., 2008. Flexural Strengthening of RC Beams with Externally Bonded CFRP Systems: Test Results and 3D Nonlinear FE Analysis. *J. Compos. Constr.* 12, 190–201.

Lee, D., Cheng, L., Yan-Gee Hui, J., 2013. Bond Characteristics of Various NSM FRP Reinforcements in Concrete. *J. Compos. Constr.* 17, 117–129.

Mugahed Amran, Y.H., Alyousef, R., Rashid, R.S.M., Alabduljabbar, H., Hung, C.C., 2018. Properties and applications of FRP in strengthening RC structures: A review. *Structures* 16, 208–238. <https://doi.org/10.1016/j.istruc.2018.09.008>

Sapulete, C.A., 2018. Studi Eksperimental Pengaruh Perkuatan Lentur Fiber Reinforced Polymer Rod pada Balok dan Efektivitasnya (thesis). Diponegoro University.

Shin, Y.S., Lee, C., 2003. Flexural Behavior of Reinforced Concrete Beams Strengthened with Carbon Fiber-Reinforced Polymer Laminates at Different Levels of Sustaining Load. *ACI Struct. J.* 100, 231–239.

Soliman, S.M., El-Salakawy, E., Benmokrane, B., 2011. Bond Performance of Near-Surface-Mounted FRP Bars. *J. Compos. Constr.* 15, 103–111. [https://doi.org/10.1061/\(asce\)cc.1943-5614.0000150](https://doi.org/10.1061/(asce)cc.1943-5614.0000150)

Tudjono, S., Lie, H.A., Gan, B.S., 2018. An integrated system for enhancing flexural members' capacity via combinations of the fiber reinforced plastic use, retrofitting, and surface treatment techniques. *Int. J. Technol.* 9, 5–15. <https://doi.org/10.14716/ijtech.v9i1.298>

Tudjono, S., Lie, H.A., Hidayat, B.A., 2015. An experimental study to the influence of fiber reinforced polymer (FRP) confinement on beams subjected to bending and shear. *Procedia Eng.* 125, 1070–1075. <https://doi.org/10.1016/j.proeng.2015.11.164>



© 2021 Journal of Geoscience, Engineering, Environment and Technology. All rights reserved. This is an open access article distributed under the terms of the CC BY-SA License (<http://creativecommons.org/licenses/by-sa/4.0/>).